

# EXTREME FATIGUE LIFE AND WEAR REDUCTION CAPABILITIES OF NI-BASED BULK METALLIC GLASS

G. Colas<sup>a\*</sup>, S. Carbillet<sup>a</sup>, A. Boucheny<sup>a</sup>, J.M. Cote<sup>a</sup>, V. Tissot<sup>a</sup>, A. Lenain<sup>b</sup>, L. Verchère<sup>b</sup>, P. Durand<sup>c</sup>, L. Cadiergues<sup>c</sup>

\*Guillaume.colas@femto-st.fr

<sup>a</sup> Université Marie et Louis Pasteur, SUPMICROTECH, CNRS, institut FEMTO-ST, F-25000 Besançon, France

<sup>b</sup> Vulkam Inc. Amorphous metal micro casting, 38610 Gières, France

<sup>c</sup> CNES, 31401 Toulouse, France

## ABSTRACT

Bulk Metallic Glasses (BMG) are known to demonstrate exceptional mechanical properties combining very high yield stress and fracture toughness with large elastic strain limit. Over the last 20 years, Ni-based and Zr based BMGs have attracted interests in gears and harmonic drives applications.

Ni-based BMG are very promising material in terms of mechanical properties ( $E = 150$  GPa,  $Y = 1280$  MPa), and corrosion properties equivalent to, or better than, 17-7 PH and 15-5 PH. Moreover, when parts are moulded, they can be net-shape because it does not shrink during cooling.

The study addressed both the fatigue life, and the wear mechanisms in rolling/sliding unlubricated contact conditions of a specific Ni-based BMG developed by Vulkam Inc. While fatigue test results are compared to the well-established literature, in tribological studies, BMG were compared to space grade 15-5 PH stainless steel. Results shows fatigue endurance higher than all commonly used alloy, and a greater wear resistance than 15-5 PH (used as reference for the tribological tests.)

## 1 INTRODUCTION

Over the last 20 years, Ni-based and Zr based BMGs have attracted interests in gears [1] and harmonic drives applications [2]. Furthermore, it has been shown that they can demonstrate high endurance fatigue life [3,4]. Although demonstrating very high potential (wear life increased by 300 times under constant torque) [5], no studies compared performances at iso-contact pressure. Indeed, at iso-resistive torque, considering the BMG Young's modulus is up to twice smaller than the regular gear steels, contact pressure becomes significantly lower.

Ni-based BMG are very promising material in terms of mechanical properties ( $E = 150$  GPa,  $Y = 2800$  MPa), and corrosion properties equivalent to, or better than, 17-7 PH and 15-5 PH [6,7]. They are also interesting because the mechanical properties are very similar to those of Ni-Fe

( $E = 160$  GPa,  $Y = 1500$  MPa) that can be used for the flexspline of harmonic drive [8]. Finally, in pure sliding condition in air, Ni-based BMG can demonstrate very low wear, even when friction coefficient is very high [9,10].

Moreover, when parts are moulded, they can be net-shape because it does not shrink during cooling. Such literature demonstrates that there is room for the use of such metallic alloy in precision mechanisms.

In this study, fatigue properties of an Ni-Based BMG, the *Vulkalloy Ni* developed by Vulkam Inc in France, has been investigated. Table 1 shows how its mechanical properties compares to those of regular alloys. The purpose was to evaluate if this alloy could be a good fit for flexure mechanism, and gear applications. As it will be presented, performances are impressive, which unlocked the second part of the project. The second part consist in evaluating the performance of the BBG in rolling with sliding contact.

Table 1 - Mechanical properties of the *Vulkalloy Ni* compared to other common alloys

	Hardness	Elast. Def	Youngs modulus	Yield strength
	HRC	%	GPa	MPa
Vulkalloy Ni	63	1.8	150	2800
TA6V	41	0.7	115	860
15-5 PH H1025	35	0.5	200	1000
440C	59	1	200	1900

## 2 EXPERIMENTAL METHODS

### 2.1 Fatigue tests

The evaluation of the fatigue endurance has been performed in 3-point bending configurations. The two extreme points were separated by 12 mm, and their radii were 2 mm. Hence, imprints on the samples were not observed. Samples' dimensions were 20 mm x 4.8 mm x

0.48 mm. Surface finish was chosen to equal  $R_a < 0.2 \mu\text{m}$  to meet the requirement imposed by the standard ISO 12107/2012 concerning Staircase fatigue testing method.

The fatigue study has been performed in three steps:

#1 Quasi-static 3-point bending test

- 5 repetitions
- Loading at 1mm/min
- Until rupture of the sample

#2 Wöhler curves

- $1.10^6$  cycles
- 30 Hz
- $R = 0.1$
- 13 tests performed

#3 Fatigue endurance under Staircase method

- $1.10^7$  cycles
- 30 Hz
- $R = 0.1$
- Step of 50 MPa
- 15 tests

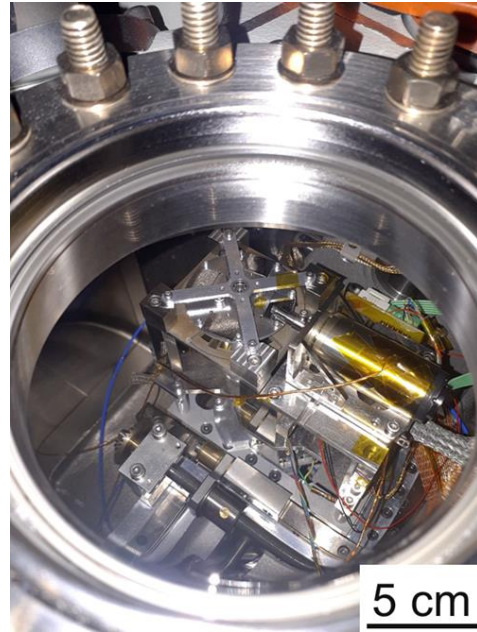
The *Vulkalloy Ni* undergone fatigue tests. Samples from two different batches have been used at each and every step. The results were then compared to the performances of most known alloys as referenced in the Metallic Materials Properties Development and Standardization (MMPDS) Handbook database.

## 2.2 Tribological studies

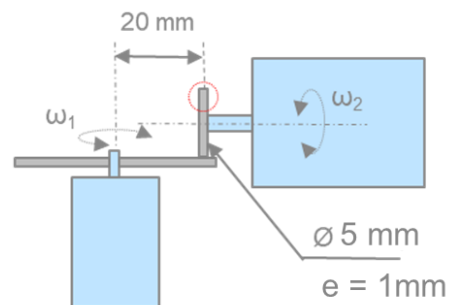
For the tribological studies, *Vulkalloy Ni* was compared to space grade 15-5 PH H1025 stainless steel. Three different contact were studied: pure BMG, pure 15-5 PH, and hybrid BMG/15-5 PH. In the latter case, the roller is made from the BMG. The maximum Hertz contact pressure considered is 750 MPa, the sliding to roll ratio is 0.6%, and the linear sliding speed is  $\sim 10.5 \text{ mm/s}$ . These test conditions were chosen to be representative of the ones encountered in typical gear train loading. 3 tests per configuration have been performed in air 50% HR, and in vacuum ( $4.10^{-7} \text{ mbar}$ ). Samples from 3 different batches of *Vulkalloy Ni* were used to make sure there is no dispersion from one batch to another. Note that due to slight time delay in the test bench control loop, short lasting pure sliding occurred at both extremities of the friction tracks.

As shown in Figure 1, due to size limitation of the available *Vulkalloy Ni* samples, oscillatory configuration has been chosen. A roller over plate configuration has been chosen. At the time of the study, only plates of *Vulkalloy Ni* were available for the study. The plate dimensions were 15 mm x 10 mm x 1mm. Roller were machined directly within the plate samples. A dedicated machining procedure has been put in place to machine

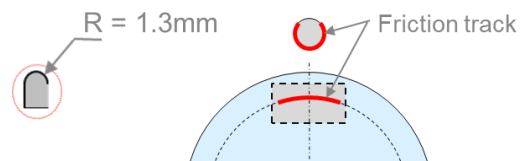
the roller with the right surface finish. To start from equivalent samples, roller in 15-5 PH H1025 have been machined from 15-5 PH H1025 plates too. The purpose was to avoid any underestimated effect from the machining.



(a)



(b)



(c)

Figure 1 - (a) picture of the tribometer used for the study, (b) and (c) scheme of the contact configuration and friction tracks

Prior to the tests, all plate samples have been mirrored polished to reach and  $R_a < 0.06$ . All roller sample geometry and surface topography have been verified under optical profilometry. Due to the size of the samples, and the curvature of the rolling track, the ISO/TR 100064-4 : Surface texture and tooth contact pattern checking has

been used to characterize the Ra and Rz parameters of the surface, in both longitudinal and transverse directions. As presented in Table 2, the roughness parameters differ from *Vulkalloy Ni* to 15-5 PH. The machining allowed to obtain better surface finish with the BMG. Nonetheless, based on the standard *ISO/TR 10064-4:1998 - Cylindrical gears Code of inspection practice Part 4: Recommendations relative to surface texture and tooth contact pattern checking*, the surface finish mostly meet the requirements for class 2 ( $Ra < 0.08$  &  $Rz < 0.5$ ) and class 3 ( $Ra < 0.16$  &  $Rz < 1$ ) gears. Only a few enters class 4 ( $Ra < 0.32$  &  $Rz < 2$ ). This means that the obtained geometries are relevant to the targeted applications.

Table 2 - roughness parameters Ra and Rz of the rollers

	Transverse		Longitudinal	
	Ra	Rz	Ra	Rz
Vulkalloy Ni	< 0.16	< 0.7	< 0.08	< 0.4
15-5 PH	< 0.3	0.1	< 0.15	< 1

After test, all samples were studied under optical microscopy and 1 set of samples (roller and plate), from each and every contact condition have been studied under SEM.

### 3 RESULTS

#### 3.1 Fatigue tests

##### 3.1.1 Quasi-static 3-point bending test

Figure 2 presents the stress/strain curves obtained from the quasi-static 3-point bending test. It demonstrates the very high reproducibility of the behaviour of the *Vulkalloy Ni*. The strain is large, and at rupture the deflection equals 2 mm. Some corrections had to be made in the data post processing to assess for such large deflection and the real distance between the two extreme holding point. With regards to the mechanical properties, the yield strength  $Re = 2842 \pm 5,3$  MPa, the ultimate strength  $Rm = 4496 \pm 74,7$  MPa, and the rupture strength is  $4233 \pm 111$  MPa.

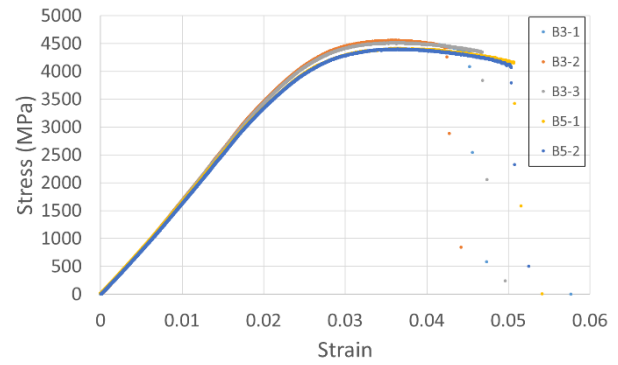


Figure 2 - Stress-strain curves from the quasi static 3-point bending test

##### 3.1.2 Wöhler curves

Figure 3 presents the number of cycles to rupture as a function of the load applied to the sample. The figures show that when the loading is above 50% of  $Re$ , the test systematically fails to reach  $1.10^6$  cycles.

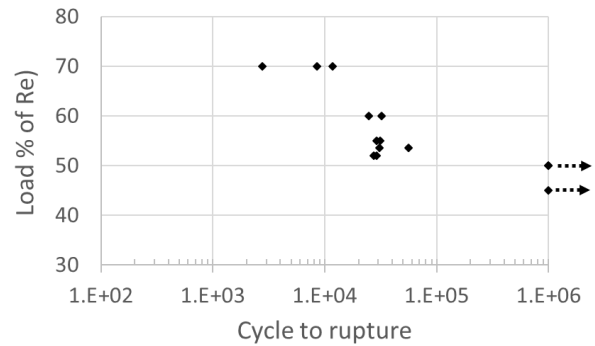


Figure 3 – S-N curve obtained from the fatigue tests according to Wöhler approach

##### 3.1.3 Endurance fatigue test (staircase method)

Table 3 presents the result from the endurance fatigue tests conducted on the *Vulkalloy Ni*. As it can be seen, the number of cycles to rupture remains lower or slightly higher than 50 000. That is in line with the binary “pass or fail” response observed with the Wöhler approach. If the test passes the ~50 000 cycles threshold, then it lasts

Table 3 - Pass and fail tests from the endurance fatigue test (@  $1.10^7$  cycles) according to the Staircase method

	Test number														
	1	2	3	4	5	6	7	8	9	10	11	12	13	14	15
	Batch number														
Stress (Mpa)	B5	B3	B3	B3	B3	B3	B5	B3	B3	B5	B3	B5	B3	B3	B5
1550			X				X								
1500		O		X		O		X		X					
1450	O					O			O		X		X		
1400												O		X	
1350															O
Cycle @ rupture			30 690	27 432			55 715	18 936		43 894	26 298		33 487	38 740	

O : passed  
X : failed

until the end of the test, i.e. it reaches  $1.10^7$  cycles.

The endurance fatigue limit at 50% reliability,  $R = 0.1$  is estimated to be  $S_{max} = 1460 \text{ MPa}$  (51%  $R_e$ ).

The standard deviation is 82MPa. This represents a relative standard deviation of 5.6%, which is consistent with that of standard alloys (typically <8%).

These results lead to  $S_{max} = 1190 \text{ MPa}$  (42%  $R_e$ ) for a 99.9% reliability.

To estimate the impact of these characteristics on the design of flexure components, it is interesting to calculate the ratio  $R_e/E$  and  $S_{max}/E$  which represent the maximum elastic strain in static and fatigue. To better compare those results with common materials, the endurance limit ratio  $S_{max}/E$  and the Yield limit ratio  $R_e/E$  have been plotted on Figure 4 for different materials (source MMPDS database).

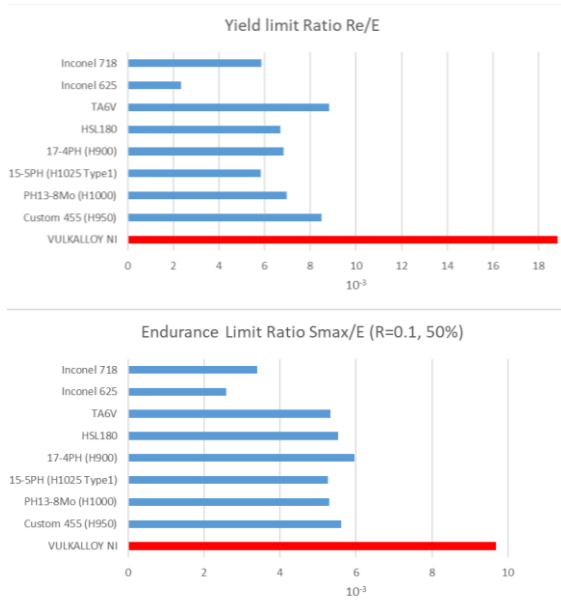


Figure 4 - Comparisons of endurance fatigue of Vulkalloy Ni with most commonly used alloys

Following the fatigue tests, samples have been observed under optical microscope. The investigation shows that the samples that pass the  $1.10^7$  cycles do not demonstrate any permanent deformation. They consequently fully retain their elasticity. For those who fail, the rupture pattern is fully in line with what is commonly observed with BMGs (Figure 5). A vein pattern is clearly detectable. The composition being fully homogeneous, when the rupture initiates (in surface mostly) it propagates straight through the thickness of the sample, leaving a vein pattern. Cracks are only visible around the neutral plan of the sample, i.e. at the frontier where compression and traction stresses are separated. That can create the well-known shear bands commonly observed in BMGs.

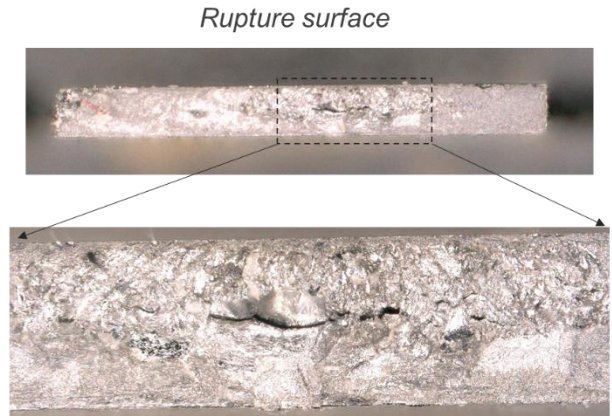


Figure 5 - cross section view of the rupture surface with a zoomed in image of the cracks and vein patterns

### 3.2 Tribological tests

The friction tests have been conducted on an in-house designed tribometer which allows for rolling+sliding experiments in a roller-on-disc contact configuration (Figure 1).

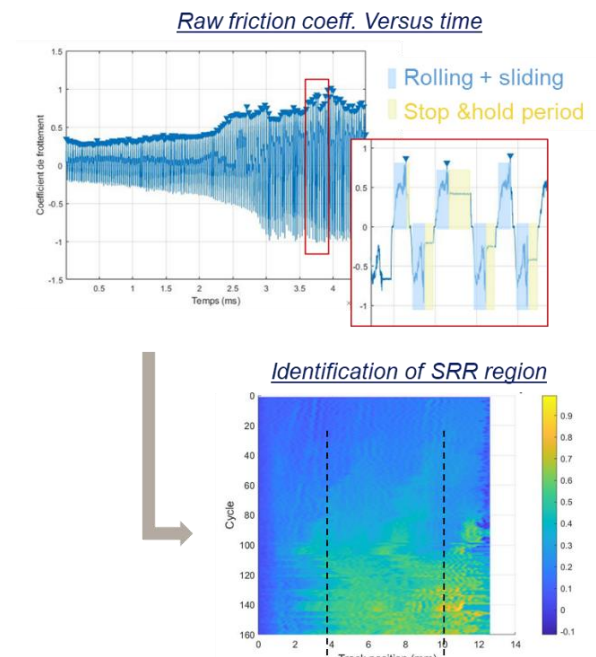


Figure 6 - Extraction of friction coefficients from rolling + sliding experiments

Due to the slight delay in the master/slave control system, pure sliding occurred at the end of each back and forth motion. On friction cycle correspond to a full back and forth motion. However, at each change of direction, there is a stop & hold period that has been shown to change from one cycle to another Figure 6. Consequently, to better post-process friction coefficient data, the raw friction data has been considered to make sure that the maximum friction peak (corresponding to pure sliding)



was not filtered. Based on the detection of this peak, pure sliding friction coefficient is linked to the maximum friction coefficient. Then the stop & hold period are detected, and finally the rolling+sliding part of the data. Due to the stiffness of the tribometer and the high friction coefficients, linear increase of friction coefficient appears prior to effective rolling+sliding. The rolling+sliding friction is then averaged on the related set of data.

Friction coefficients are displayed on Figure 7. Note that only one curve of friction per configuration is shown, all 3 tests per configurations are very similar. It is interesting to note that there are differences in the classification of friction between max and mean friction coefficients, i.e. between pure sliding or rolling+sliding. Friction coefficient can reach very high level but also very low one depending on the configuration and the environment.

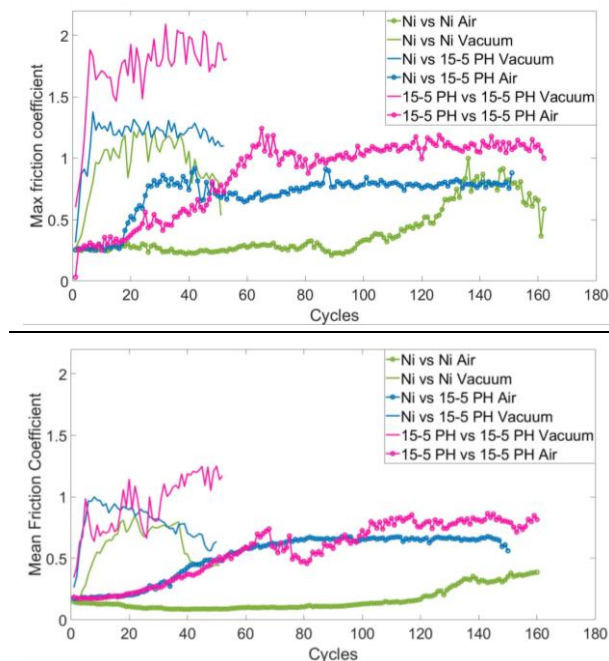


Figure 7 - Max friction coefficient (pure sliding case) and mean friction coefficient (rolling + sliding case) of the 3 different contact configurations in both humid air and vacuum

Regarding the max friction coefficient (pure sliding), in vacuum, the fully BMG and hybrid contacts are equivalent. Although one can note a dome like friction curve for the fully BMG contact, which may lead to lower friction if the test was run longer. The fully 15-5 PH contact is the worst with significantly higher friction. In air, the best behaviour is obtained with the fully BMG contact, with a max friction reasonably low, around 0.3, over a long period of time. The hybrid contact is in second place with a sharp increase in friction, early around 20 cycles. However, it stabilizes around

moderately high friction coefficient (0.8), which happens to be the same level of high friction from fully BMG contact. Then comes the worst case, the fully 15-5 PH whose friction rises gradually over the 60 first cycle to reach the highest level of friction in air, around 1.

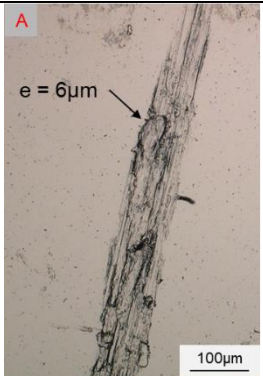
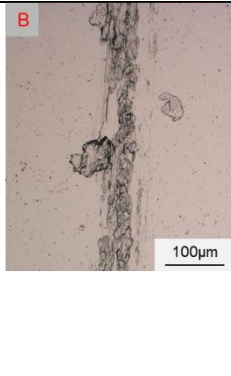
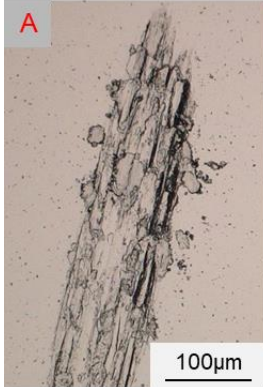

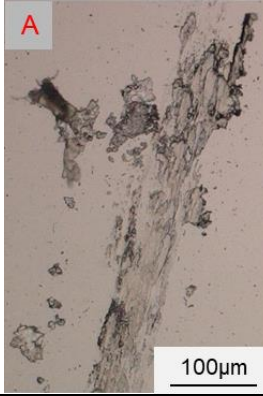
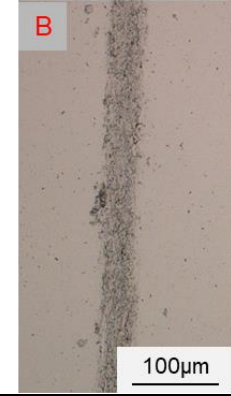
In rolling+sliding (mean friction coefficient), in vacuum, the friction coefficient level is equivalent for all 3 contacts during the first 20 cycles. Then, both fully BMG and hybrid contacts demonstrate a decrease of friction, while the friction coefficient of the fully 15-5 PH contact keeps increasing. In air, the fully 15-5 PH and hybrid contacts are showing the same trends, they are superimposed. However, the hybrid contact appears more stable. The stable friction reach for the hybrid contact is 0.6, while it is 0.7 for the fully 15-5 PH contact. The fully BMG contact is demonstrating low friction coefficient (0.1) during the first 120 cycles. It then rises to reach a mean value of 0.3-0.4.

In terms of surface damage, the differences are somewhat subtle between the 3 configurations, in vacuum. The fully 15-5 PH demonstrates the presence of large agglomerates resulting from adhesive wear and extrusion of the material under friction. Those agglomerate can be thick, above  $5\mu\text{m}$  and up to  $10\mu\text{m}$ . Adhesive wear is observed, particularly in the pure sliding region. In centre track, under rolling+sliding, damages are more local, but large agglomerates are observed. The hybrid contact demonstrates narrower tracks, but adhesive wear is still observable through the presence of extruded material, and of few agglomerates, in the pure sliding region. The centre track is showing local plastic deformation but homogeneously distributed over the whole track. The full BMG contact exhibits the narrower tracks. In pure sliding region, it appears that sheets/ribbon-like particles are observed. Damages are localized on top of the surface, and they are moderate. Under rolling+sliding (centre track), similar features than the hybrid contact are observed, but they are much smaller, the track is at least twice narrower than the track of both the hybrid and fully 15-5 PH contacts.

In air, the surfaces morphologies are exhibiting significant differences between the 3 different contact configurations. The fully 15-5 PH contact is exhibiting very large wear, and the widest tracks. The presence of deep abrasion grooves is easily observable. There is a significant amount of loose particles inside and around the tracks, in both pure sliding and rolling+sliding region. The hybrid contact is interesting because there is a significant difference of track between the 2 regions. In the pure sliding region, grooves resulting from abrasion can be seen. And there are few particles in this region too. In the rolling+sliding region, no groove is detected, and particles are rarely detected. What both regions have in common is the presence of a thick dark 3<sup>rd</sup> body layer. Finally, the fully BMG contact demonstrate extremely

low wear in both pure sliding, and rolling+sliding regions. In pure sliding region, few thin agglomerates are detected, it is plasticized material with a morphology that is closed to what is observed in vacuum. However, that is the only thing observable as the surface around these agglomerates appears to remain pristine. In the rolling+sliding region, damages are only local, and larger areas remains untouched or with undetectable surface modifications. There appear to be dotted tracks. Damages are very local and localized at the top surface of the plate.


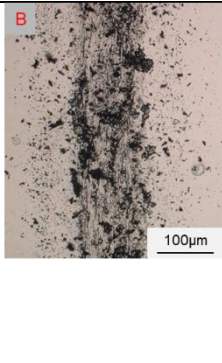


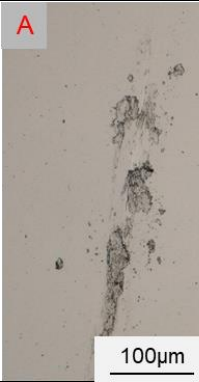
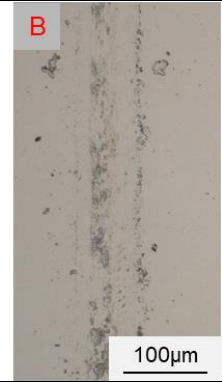
Table 4 - Optical images of the friction track, on the plate sample, after test in vacuum. A is one extremity in pure sliding, and B is the centre of track rolling+sliding

Fully 15-5 PH	 
Hybrid	 
Fully BMG	 

The rollers are not shown here but they have been investigated too. The wear patterns fully reflect those

observed on the plates, except for the hybrid contact in air. In the hybrid case, the roller in the BMG *Vulkalloy Ni*. In air, the wear of the BMG roller in the hybrid case is similar to the roller from the fully BMG contact. Consequently, the dark materials most likely comes from the 15-5 PH, or most likely contains material coming from the 15-5 PH.

Table 5 - Optical images of the friction track, on the plate sample, after test in vacuum. A is one extremity in pure sliding, and B is the centre of track rolling+sliding

Fully 15-5 PH	 
Hybrid	 
Fully BMG	 

#### 4 CONCLUSION

In this study both the fatigue life, and the wear mechanisms in rolling/sliding unlubricated contact conditions of a specific Ni-based BMG, have been investigated. The Ni-based BMG tested is the Vulkalloy Ni.

The endurance fatigue test showed that the endurance fatigue limit at 50% reliability,  $R = 0.1$ , is estimated to be  $S_{max} = 1460 \text{ MPa}$  with  $\pm 82 \text{ MPa}$  of standard deviation.  $S_{max} = 1190 \text{ MPa}$  for a 99.9% fatigue reliability. That means Vulkalloy Ni surpasses all the reference materials (Inconel, TA6V, etc.). That makes it extremely promising material for flexure applications as it can accept larger elastic strain than crystalline material.

A next step will be the evaluation of Vulkalloy-Ni blades for the LOVBB (Lunar Optical Very Broad Band) seismometer. LOVBB is currently developed by IPGP (Institut de Physique du Globe de Paris) and CNES [11]. It is mechanically based on the principle of an inverted pendulum (Figure 7). A proof mass rotates around a flex pivot. A spring balances the weight momentum. When a ground vertical motion occurs, the pendulum is excited.

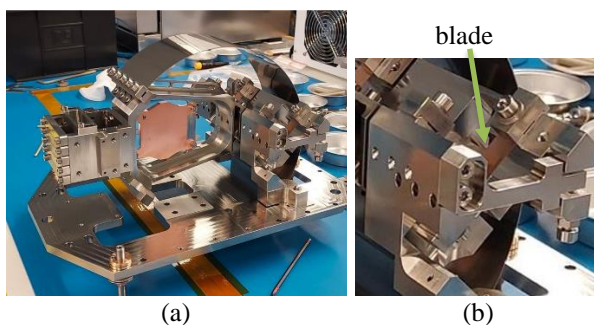


Figure 8 - (a) LOVBB Mechanical oscillator, (b) zoom on the flex pivot

During the launch, the mobile part of the pendulum will be locked. But because of the hyperstatic configuration during this phase, part of the load must be supported by the pivot and its blades. The high Re/E ratio of Vulkalloy-Ni is therefore of great interest for this application, as it allows the optimization of launch load capacity while maintaining the level of pivot flexibility required for seismometer performance.

The tribological test performed at iso contact stress, shows that the *Vulkalloy Ni* surpasses 15-5 PH H1025 in the tested contact conditions. Hybrid contact have been tested, and their performances lie between fully 15-5 PH and fully *Vulkalloy Ni* contacts. The latter shows stable and repeatable friction, the longest low friction life. It is the only one to demonstrate low wear in both air and vacuum, only few loose particles are observed. The study also shows that iso contact stress, in microgear box, means  $\sim 2x$  resistive torque with BMG as compared to regular steel. Hence, higher acceptable torque is possible at iso dimension. Or, for iso torque, longer life is highly expected. It is also possible to further push miniaturization of gearboxes.

The study showed that Vulkalloy-Ni is a promising candidate for tribological applications. Further study is

expected to pursue the investigation in lubricated conditions.

## 5 ACKNOWLEDGMENT

The authors wish to thank the French space agency (CNES) for supporting the study. They also thank the French RENATECH network and its FEMTO-ST technological facility for the access to analysis instruments, and the EIPHI Graduate School. Finally, they thank the experimental platform AMETISTE, for the access to the optical profilometer, and the microfabrication platform MIFHySTO.

## 6 REFERENCES

- [1] Ishida M, Takeda H, Nishiyama N, Kita K, Shimizu Y, Saotome Y, et al. Wear resistivity of super-precision microgear made of Ni-based metallic glass. *Mater Sci Eng A* 2007;449–451:149–54. <https://doi.org/10.1016/j.msea.2006.02.300>.
- [2] Hofmann DC, Polit-casillas R, Roberts SN, Borgonia J, Dillon RP, Hilgemann E, et al. Castable Bulk Metallic Glass Strain Wave Gears: Towards Decreasing the Cost of High-Performance Robotics. *Sci Rep* 2016;6:1–11. <https://doi.org/10.1038/srep37773>.
- [3] Jia H, Wang G, Chen S, Gao Y, Li W, Liaw PK. Fatigue and fracture behavior of bulk metallic glasses and their composites. *Prog Mater Sci* 2018;98:168–248. <https://doi.org/10.1016/j.pmatsci.2018.07.002>.
- [4] Fujita K, Zhang W, Shen B, Amiya K, Ma CL, Nishiyama N. Fatigue properties in high strength bulk metallic glasses. *Intermetallics* 2012;30:12–8. <https://doi.org/10.1016/j.intermet.2012.03.021>.
- [5] Inoue A, Shen B, Takeuchi A. Fabrication, properties and applications of bulk glassy alloys in late transition metal-based systems. *Mater Sci Eng* 2006;441:18–25. <https://doi.org/10.1016/j.msea.2006.02.416>.
- [6] Inoue A, Nishiyama N. New Bulk Metallic Glasses for Applications as Magnetic-Sensing, Chemical, and Structural Materials. *MRS Bull* 2007;32:651–8.
- [7] Hampson M. ESA-ESTL-TM-0153 01- Gear Materials Review. 2015.
- [8] Slatter R, Degen R. Miniature zero-backlash gears and actuators for precision positioning

applications. Proc 11th Eur Sp Mech Tribol Symp - ESMATS 2005 2005:9–15.

- [9] Colas G, Marco C, Lucas D, Imhoff L, Heintz O, Lenain A, et al. Tribochemistry dependence of Ni<sub>62</sub>Nb<sub>33</sub>Zr<sub>5</sub> bulk metallic glass on the Cr content of steel counterparts. Tribol Int 2024;198. <https://doi.org/10.1016/j.triboint.2024.109923>.
- [10] Cornuault P-H, Colas G, Lenain A, Daudin R, Gravier S. On the diversity of accommodation mechanisms in the tribology of Bulk Metallic Glasses. Tribol Int 2020;141:105957. <https://doi.org/10.1016/j.triboint.2019.105957>.
- [11] Gabriel Pont and al. "Lunar Seismometers: Past, Present and Future". IAC-2024,A3,2B,10,x85876,